Precision Measurements of Nuclear γ-Ray Wavelengths of Ir^{192}, Ta^{182}, RaTh, Rn, W^{187}, Cs^{137}, Au^{198}, and Annihilation Radiation*

DAVID E. MULLER, HARRY C. HOYT, DAVID J. KLEIN,† AND JESSE W. M. DUMOND
California Institute of Technology, Pasadena, California

(Received July 14, 1952)

The sensitivity of the curved crystal gamma-ray spectrometer has been improved (1) by replacing the multicellular Geiger counter formerly used as a detector with a sodium iodide crystal scintillation counter and (2) by doubling the thickness of the quartz crystal which is used for diffraction of gamma-rays. Certain minute nonlinearities in the spectrometer have been detected and corrected in a recent calibration. An analysis of the precision of the instrument based on this calibration and a systematic treatment of errors due to random variations in counting rate is presented. Verification of the quoted precision is achieved by comparisons of wavelengths measured in various orders and by consistency of Ritz combinations.

Precision measurements of the wavelengths and energies of nuclear gamma-rays and x-rays which follow the decay of iridium 192, tantalum 182, radiothorium, radon, tungsten 187, cesium 137, and gold 198, as well as the annihilation radiation from copper 64, are tabulated. A topological system is used to enumerate all possible level schemes agreeing with a given set of Ritz combinations. This method is applied to determine possible level schemes for iridium 192 and tantalum 182. After all corrections, the measured wavelength of the annihilation radiation from copper 64 agrees, within the precision of the measurements, with the present "best" value of $h/m_e c$ (for electrons) as obtained by entirely independent methods. It is concluded that to a part in 10^4 there is no evidence for any difference in mass between positive and negative electrons.

I. INTRODUCTION

METHODS of measuring gamma-ray energies have advanced in two directions in the past few years. Much progress has been made in the measurement of extremely weak gamma-rays by the use of scintillation spectrometers of the type used by Hofstadter.[1] On the other hand, the method of crystal diffraction has been used to obtain highly precise measurements of relatively intense gamma-rays. Measurements of the latter type were made from 1947 to 1949 on a number of gamma-rays with the focusing crystal gamma-ray spectrometer of DuMond,[2–5] although at this time it was possible to obtain few sources of gamma-radiation in sufficient specific activity to allow measurements. Since then neutron irradiated sources of much higher specific activity have become available to us through the use of reactors with higher neutron flux than that available at Oak Ridge. Furthermore, the sensitivity of the spectrometer itself has been improved manyfold (1) by replacing the multicellular Geiger counter previously used for detecting the gamma-rays[6] with a sensitive scintillation counter using a thallium-activated sodium iodide crystal, and (2) by use of a 2-mm thick quartz crystal for diffracting the gamma-rays instead of a 1-mm crystal. Through such improvements in sensitivity and luminosity, a large number of gamma-rays which previously lay beyond the reach of this precise method may now be measured directly.

The scintillation counter which is employed as a detector contains a rectangular 3×3×1 in. single sodium iodide crystal as the scintillating element, so placed that it intercepts the 3×3 in. gamma-ray beam which is reflected from the quartz crystal. In order to protect the sodium iodide from the effects of the moisture in the air, it is immersed in a medium of resin and enclosed in a glass box. Scintillations from this crystal are detected by means of two RCA 5819 photomultiplier tubes making optical contact with two opposite 3×1 in. faces of the crystal through Plexiglas light conductors. These photomultipliers are operated in coincidence so as to reduce the amplitude of the random shot noise from the photomultipliers which, were it not reduced in this fashion, would produce pulses in the counting circuit similar to those produced by low energy gamma-rays. A drawing of the assembly of two photomultiplier tubes and scintillation counter, the latter with the front cover removed, is shown in Fig. 1.

Pulses from the coincidence circuits whose magnitudes fall within a chosen range are selected by means of adjustable upper and lower pulse-height discriminators, thus providing a means of rejecting pulses due to cosmic rays (which are generally very large) and some unwanted gamma-rays. As will appear later, this pulse-height discriminator also serves the valuable purpose of identifying the crystal order in which a line is reflected since it yields independent information regarding line energies.

II. CALIBRATION OF THE SPECTROMETER

Since the curved crystal spectrometer is designed primarily to achieve high precision, it is of importance to include here a rather detailed description of (1) the most recent calibration which makes this precision

* This work was performed and financed under the joint sponsorship of the ONR and AEC by contract with the California Institute of Technology.

† Now with North American Aviation, Inc., Downey, California.

[1] J. A. McIntyre and R. Hofstadter, Phys. Rev. **78**, 617 (1950).

[2] DuMond, Lind, and Watson, Phys. Rev. **73**, 1392 (1948).

[3] DuMond, Lind, and Watson, Phys. Rev. **75**, 1226 (1948).

[4] Lind, Brown, Klein, Muller, and DuMond, Phys. Rev. **75**, 1544 (1949).

[5] Lind, Brown, and DuMond, Phys. Rev. **76**, 1838 (1949).

[6] D. A. Lind, Rev. Sci. Instr. **20**, 233 (1949).

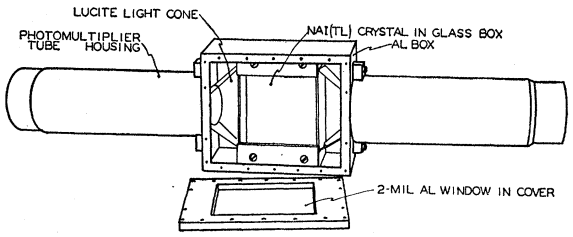

FIG. 1. The scintillation counter with front cover removed, exposing the crystal.

possible, and (2) certain auxiliary optical equipment which has recently been installed to permit correction for certain mechanical flexures in parts of the instrument.

An illustration of the basic geometry of the curved crystal spectrometer may be seen in Fig. 2. The crystal used for diffraction of the gamma-rays, which is shown schematically at C, consists of a slab of quartz 2 mm thick. It is bent elastically so that its (310) atomic planes, which are normal to the face of the crystal, converge toward the point β, 2 meters away. The reason for bending the crystal in this way is to allow all rays from a line source of gamma-radiation at R to make the same angle θ with the crystal planes, thus making use of the entire crystal at once. It may be seen from simple geometry that this is approximately accomplished as long as the source R lies on the circle passing through C and β and having a center at O. This imaginary circle on which the source R must lie is called the focal circle.

Reflection of gamma-rays from the crystal planes occurs when θ equals the Bragg angle for the radiation being studied. Since the reflected radiation leaves the crystal planes at the angle of incidence, it diverges as though it were coming from the virtual focus point V. This divergent beam is separated from the heterogeneous radiation passing directly through the crystal by means of the tapered lead sheets (called the collimator) at A, and is detected by the scintillation counter at G.

The mechanism of the spectrometer shown in the perspective line drawing of Fig. 3 is designed to serve three purposes. (1) It permits accurate measurement of the sine of the angle θ, which is the Bragg angle whenever reflection occurs. (2) It constrains the source R to move on the focal circle, thus satisfying the focusing condition. (3) It moves both source and crystal in such a way that the Bragg reflected radiation remains fixed in space. This feature makes it unnecessary to move the heavy collimator and detector shown at A and G.

In Fig. 3 the crystal is shown at C, while the source in its lead shielding lies at R. Those elements of the mechanism which rotate with the crystal frame of reference are (1) the lower beam F, which is connected to the crystal by means of a shaft; (2) the center of the focal circle O, lying on F; (3) the swinging track T, which pivots about the point V'; (4) the long carriage Q which is driven on the track T by a screw in the lower part of Q. Q is prevented from rotating with respect to F by means of a $1\frac{1}{4}$-inch rod B' terminating F, which passes in and out through bearings on either side of Q in a direction perpendicular to the motion of Q.

In order that the reflected radiation remain fixed in space, the source R and the source beam U upon which it rides must rotate about the crystal pivot at twice the angular speed of the crystal. This is accomplished by driving the small carriage L (which supports U) along Q at the same rate that Q is being driven on T. L is driven by means of a precision screw in the upper part of Q having the same pitch as the lower screw which is geared directly to it. While the upper beam U is moving, the source R travels lengthwise on U so as to stay on the focal circle to which it is constrained by the radius arm OR.

Since the beam F is held perpendicular to the direction of travel of Q and L, it is possible to measure a distance proportional to the sine of the angle of incidence with the precision screw. Thus a scale proportional to wavelengths can be read directly in terms of rotation of the screw because of the form of Bragg's

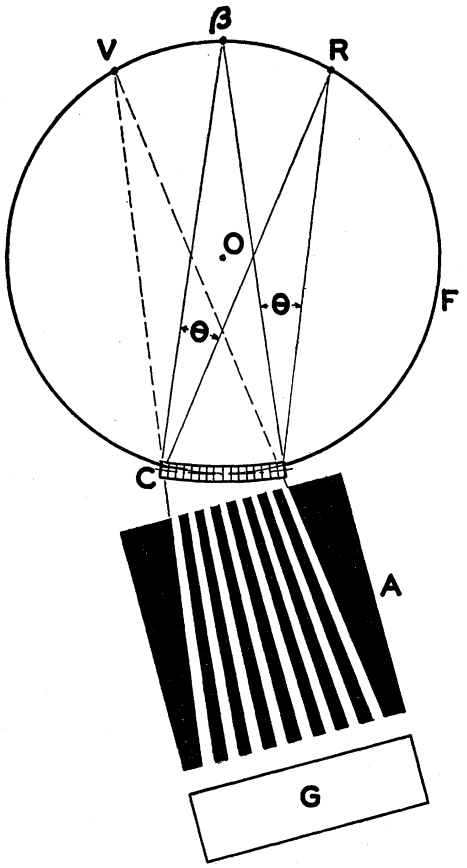

FIG. 2. Basic geometry of the gamma-ray spectrometer. The crystal appears at C and the source at R on the focal circle F. The reflected radiation appears to diverge from the virtual focus V as it passes through the collimator A to the detector at G.

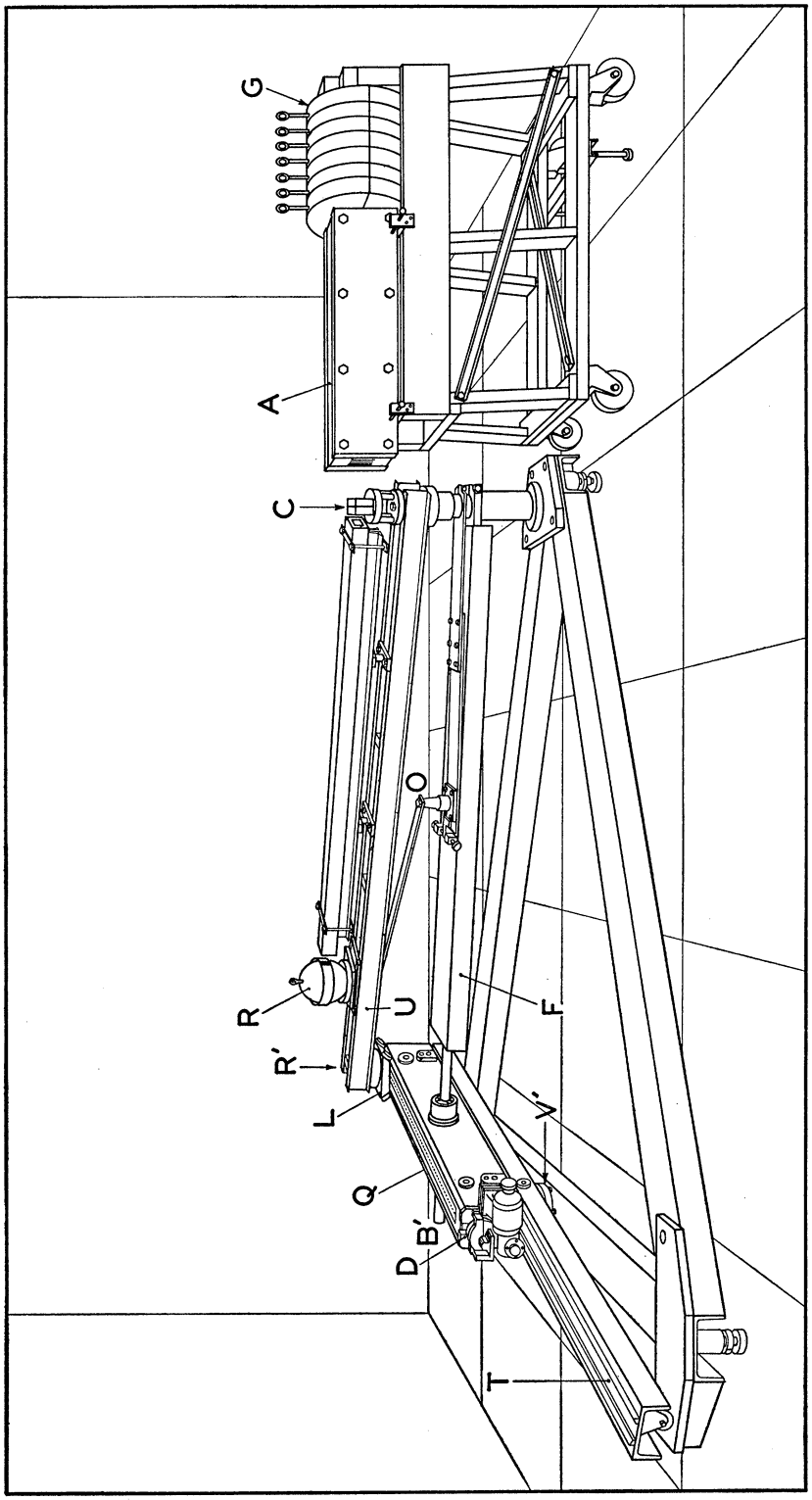

FIG. 3. Perspective line drawing of the gamma-ray spectrometer showing the curved crystal at C and the source in its shielded holder 2 meters from it at R.

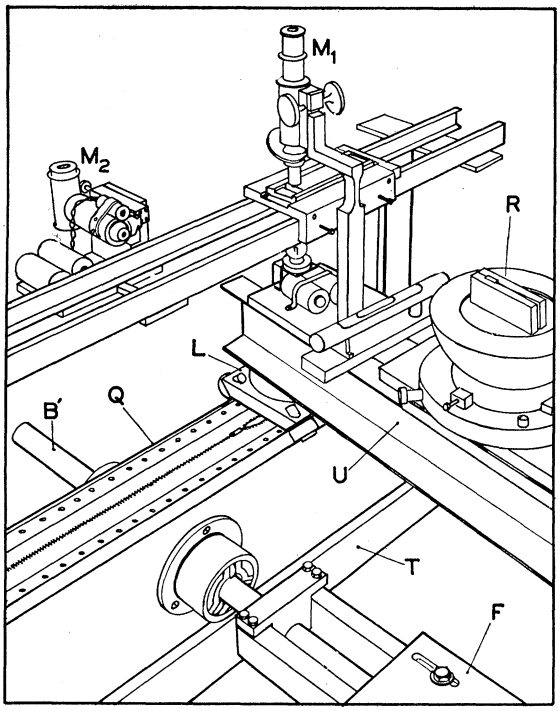

FIG. 4. Arrangements for the calibration of the spectrometer. A pair of rails rigidly supported on the long screw carriage carry a small carriage provided with a Bureau of Standards calibrated precision glass scale. A vertical microscope M_1, rigidly attached to the upper (source supporting) beam U, views the glass scale. The focus of the microscope is at the same height as the source R and is directly above the pivot of the small carriage L, supporting the upper beam. The horizontal elbow microscope M_2 and tiny light source used in conjunction with the 6-inch concave mirror to detect any anomalies in the motion of the crystal pivot are mounted at the center of the rails. The source holder R, standing on the lower half of the lead bomb used for shielding, can be seen at the right center.

law, $n\lambda = 2d \sin\theta$. Gamma-ray wavelengths are measured by comparing the positions of the line profiles taken *on opposite sides* of the central source position, thus eliminating the need for a well-defined zero on the machine.

To calibrate the instrument, it is necessary to check as completely as possible that the screw measurements do correspond to the sine of the angle of incidence of the gamma-radiation on the curved crystal. This is done in a two-step procedure.

First, precision displacements, measured with respect to the long carriage Q, of a point defined by the focus of a microscope vertically above the pivot R' and rigidly fixed to the source beam at the same height as the source, were calibrated against rotation of the screw, and second, the deflections of the curved crystal C with respect to a point fixed in the system Q were studied. In this way a complete check on the motion of the source with respect to the crystal was made.

In order to carry out the first mentioned part of the calibration, a framework to support a pair of steel rails was built on the long carriage Q. A 100-power microscope, M_1, mounted exactly above the pivot R' on a bracket rigidly attached to the source beam was used to observe the scratches in a Bureau of Standards calibrated glass decimeter scale which was set on these rails (see Fig. 4). By setting the glass scale at particular positions on the rails and reading the screw positions corresponding to various scratches on the glass scale, it was possible to calibrate the precision screw. Care was taken to make sure that the height on the instrument at which the scratches were observed was the same as the mean height of the gamma-ray source. Thus any reproducible minute rocking of the source beam (around its long axis), because of departures from straightness in the ways, for example, would be corrected in the calibration.

For the second mentioned part of the calibration, in which a check was made on the alignment of the crystal with an invariable point fixed on the long carriage, a 6-inch spherical concave mirror having a 90-inch radius of curvature was mounted in place of the curved crystal, and with its center of curvature located centrally on the long carriage at the height of the source. A second 100-power microscope M_2 visible in Fig. 4 was mounted on the framework, which had been built on the long carriage in such a position that its focus was located just below the center of curvature of the 6-in. mirror, while a tiny set of cross hairs, illuminated from behind, was mounted just above the center of curvature. In this way the image in the 6-in. mirror of the cross hairs

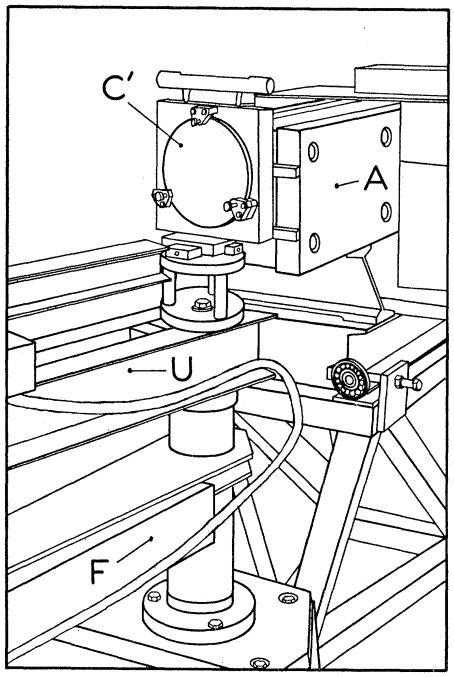

FIG. 5. The 6-inch precision-figured concave mirror C', mounted on the crystal pivot in place of the crystal, where it served, along with the elbow microscope M_2 and light source of Fig. 4, to check the fidelity with which the turning of the crystal pivot followed the motion of the long screw carriage.

appeared at the focus of the second microscope. Slight angular motions of the crystal pivot with respect to the long carriage, produced by flexures in the parts of the spectrometer, were measured by observing deflections of the image of the cross hairs on a scale located in the eyepiece of the second microscope. By observing the image of the cross hairs at approximately the height of the gamma-ray source, the sine of the angle of incidence of gamma-rays on the curved crystal may be measured to an accuracy of about 10^{-6} independently of slight tilts of any of the carriages or pivots. In Fig. 4 may be seen the calibration framework and microscopes, while in Fig. 5 the 6-inch mirror may be seen mounted above the crystal pivot.

Since the glass decimeter scale would only cover $\frac{1}{10}$ of the one meter screw at a time, it was necessary at intervals to slide the scale along the rails, while maintaining the spectrometer in a fixed position, and match the terminal scratches on the scale. In this way the entire screw was calibrated in steps of one decimeter.

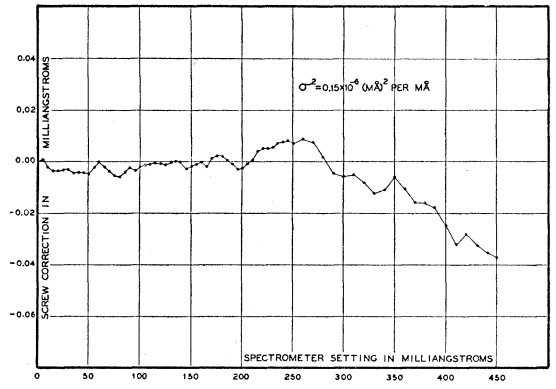

FIG. 6. The wavelength correction necessitated by nonlinearity of the screw. Quasi-periodic correction has been subtracted.

Within each decimeter, points were taken either every 5 or every 10 millimeters, depending on the region being calibrated. In addition to this over-all calibration, the deviations from linearity of the screw which occur in single revolutions of the screw were studied by replacing the decimeter scale with a second calibrated glass scale having scratches every tenth of a millimeter over a distance of one millimeter. Such single revolutions were calibrated every ten revolutions within the interesting range and a quasi-periodic error was thus eliminated.

Results of both the screw calibration and the alignment of the crystal with the long carriage are plotted in Figs. 6 and 7, respectively. Both of these corrections are zero at 208.996 milliangstroms, the wavelength of the tungsten $K\alpha_1$ x-ray line, since this line, which has been measured with high precision,[7] is used for fixing the scale of the screw in terms of wavelength units and therefore represents a known point on the screw. An inspection of these curves shows that the latter

[7] Watson, West, Lind, and DuMond, Phys. Rev. **75**, 505 (1949).

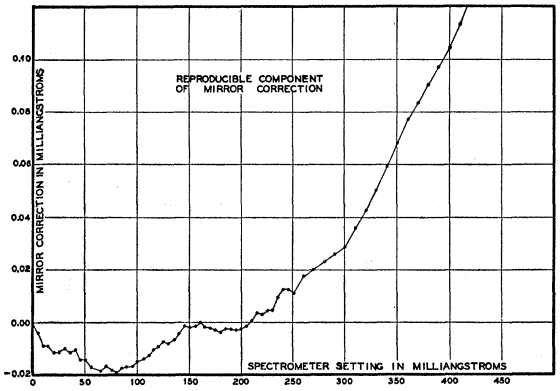

FIG. 7. The wavelength correction necessitated by misalignment of the crystal with the long carriage.

correction (the one observed with the concave mirror) is by far the greater. We have shown that it is chiefly due to two influences: (1) a slight variable flexure of the $1\frac{1}{4}$-inch rod which terminates the lower beam (B', Fig. 4), and (2) minute flexures in the base of the instrument (caused by the shifting of the weight of the screw carriage, as the wavelength scale is explored, which tilts the crystal pivot (in a nonlinear way) clearly detectable by the sensitive level mounted on top of the six inch mirror. That part of the correction due to the flexure of the $1\frac{1}{4}$-inch rod has been entirely explained by an analysis of the effects of known forces and torques which are present in the instrument. We have also observed that this "mirror correction" exhibits considerable hysteresis, i.e., its magnitude depends on the history of the sequence of wavelength settings which have been made just previous to the observation. This is undoubtedly due to nonreproducible flexure of the $1\frac{1}{4}$-inch bar which determines the orientation of the long carriage Q and the track T. The combined correction plotted in Fig. 8 shows, furthermore, that within the range of settings corresponding to gamma-ray wavelengths, this correction is never greater than 0.025

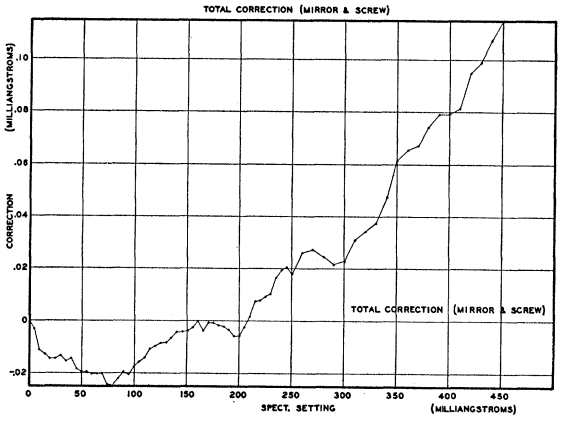

FIG. 8. The sum of screw and mirror corrections, representing therefore the total correction to be applied to measurements in the range of wavelengths from 0 to 450 milliangstroms.

TABLE I. Wavelengths (in milliangstroms) of five intense lines from iridium 192 as measured in various orders after being corrected using the older, inferior calibration which ignored the "mirror-correction."

Energy, kev	3rd order	2nd order	1st order
295.94	41.898	41.894	41.909
308.45	40.191	40.205	40.214
316.46	39.174	39.183	39.197
467.98	26.496	26.503	26.515
Iridium $K\alpha_1$ x-ray		190.993	191.025

milliangstrom. To visualize the minuteness of these corrections, one must realize that 0.02 milliangstrom corresponds to a motion of the gamma-ray source of less than 0.02 millimeter, or to a deviation in the sine of the Bragg angle of less than 10^{-5}.

In our earlier work with this instrument up to the spring of 1951, we had indeed corrected for periodic and aperiodic errors in our screw, but these calibration curves were much less carefully observed and also took no account of the then unsuspected "mirror correction." The scale in this earlier calibration was, furthermore, not supported at the same height as the source so that the calibration did not correct for minute rocking of the source beam.

The first definite internal evidence of slight residual nonlinearity in our supposed linear wavelength scale came when, thanks to greatly improved sensitivity secured by replacing our earlier "multicellular" Geiger counters with a sodium iodide scintillation crystal, we were able to observe one and the same wavelength in three different orders of reflection from the curved quartz crystal for four different intense nuclear gamma-ray lines emitted by an exceptionally strong source of iridium 192. We were also able to observe the intense $K\alpha_1$ x-ray line from iridium in first- and second-order reflection. These results (see Table I) exhibited a very definite systematic trend: Wavelengths computed from higher order reflections were (in every case but one) slightly shorter. These disagreements, however, were not sufficient to establish a very reliable correction curve by themselves. Nevertheless, it was because of them that the intensive recalibration and study of the minute causes of nonlinearity in the instrument (lasting over a period of six months) was undertaken.

An idea of the reliability of the new calibration may be gleaned from a comparison of the intense lines of iridium 192 which were measured in first, second, and third orders. These results, which are compared in Table II after making the new calibration correction and the mirror correction, agree well within their assigned errors and correspond to measurements made at one, two, and three times the wavelength settings of these lines. It is interesting to note that even the measurements on the intense iridium $K\alpha_1$ line, which was obtained in the second as well as the first order, agree quite well in spite of the fact that corrections in this case were relatively large.

At present the calibration equipment is to be used to provide still higher precision than was possible before. By permanent installation of the 6-inch mirror above the curved crystal, the alignment of the crystal with the long carriage is now and henceforth checked at the time and every time that the gamma-rays are actually being measured. In this way, any possible hysteresis or nonreproducibility present in this motion is automatically taken into account. Similar methods are used for checking the behavior of the screw.

With the use of these improvements a further exceedingly satisfactory check has been made on the reliability of the calibration by observing in three different orders of reflection the 412-kev line from a strong source of gold 198. Wavelength measurements in the first, second and third orders of reflection are 30.102 ± 0.0038, 30.105 ± 0.0033, and 30.107 ± 0.0028 milliangstroms, respectively. Disagreement between these measurements lies well within the assigned errors, thus confirming even more satisfactorily the reliability of the calibration. This is definitely not the case in the data obtained before the screw calibration and mirror corrections were applied.

By making multiple calibrations of the spectrometer, it was possible to estimate the errors which arose during the calibration. This was done by determining the mean square deviations from the mean and dividing by the number of degrees of freedom. A random walk analysis of the over-all calibration of the screw was used to determine the error of the calibration. For this part of the calibration $\sigma^2 = 0.15 \times 10^{-6} (\text{mA})^2$ per mA. A determination of the errors in the quasi-periodic calibration was accomplished by repeating the calibration of single turns of the screw. Random variations in screw readings and in the "mirror correction" were treated in a similar fashion. Results of these calculations indicate that the errors to be expected in wavelength measurements made subsequent to the calibration are less than 0.005 milliangstrom because "mirror" readings are taken at the time the gamma-rays are measured. Measurements made prior to the calibration are subject to the somewhat larger uncertainty of about 0.01 milliangstrom because no check had been made at that time of the alignment of the crystal with the long carriage. In order to correct these older measurements the curve shown in Fig. 7 (which was obtained during the calibration) had to be used.

TABLE II. Wavelengths (in milliangstroms) of five intense lines from iridium 192 as measured in various orders after being corrected using the latest calibration.

Energy, kev	3rd order	2nd order	1st order
295.94	41.891	41.885	41.887
308.45	40.187	40.190	40.191
316.46	39.172	39.172	39.175
467.98	26.486	26.491	26.495
Iridium $K\alpha_1$ x-ray		191.041	191.031

Theory of Errors in Wavelength Measurement Resulting from Random Variations in Counting Rate Alone

For wavelength measurement, plots are made of the two line profiles obtained by use of internal reflection from opposite sides of the crystal planes. A typical pair of such plots is shown in Fig. 9. Since the wavelength of the line corresponds to the number of screw divisions of displacement between such opposite plots, the following system has been devised for determining such displacement with high precision. A composite line profile is drawn from the superposition of several such plots. This composite line profile is then matched as carefully as possible to the two opposite plots of a line. By measuring the displacement of this composite profile in going from one plot to the opposite one, a measurement of wavelength can be made with an error which is a small part of the actual breadth of a line.

In order to analyze the error[8] resulting from the above procedure, it is necessary to derive an expression for the precision with which a composite profile can be fitted to the plot of a line, assuming that a least squares fit is obtained.[9] Let $L(u)$ be the average counting rate at spectrometer setting u. $L(u)$, therefore, represents a line profile if u covers a range of settings which include a line. If a series of measurements of counting rate is made lasting τ minutes each at a set of positions u_i, $i=1, \cdots, n$ the expected number of counts at each point will then be given by $\tau L(u_i)$, and the standard variation of each such point from its expected number of counts will be $[\tau L(u_i)]^{\frac{1}{2}}$ if the normal distribution is used to approximate to the Poisson distribution. Each counting rate measurement at a point u_i may be thought of as constituting an independent measurement of the position of the composite profile, since the profile, once obtained, could conceivably be fitted to a single point. As such, the standard error of the position measurement corresponding to a run at u_i lasting τ minutes is $[\tau L(u_i)]^{\frac{1}{2}}/\tau L'(u_i)$, provided that the slope $L'(u)$ of the curve $L(u)$ does not change appreciably over the vertical interval $[\tau L(u_i)]^{\frac{1}{2}}$, so that the error in fitting the composite profile horizontally may also be considered normal. The combined effect of the measurements of counting rate at all n points can be regarded as a combination of independent measurements, each contributing with a weight inversely proportional to the square of its standard error. Hence, if σ is the standard error of the fitting of the composite profile to all points, we obtain

$$1/\sigma^2=P=\sum_{i=1}^{n}\tau[L'(u_i)]^2/L(u_i). \tag{1}$$

$P=1/\sigma^2$ is a convenient measure of the precision of fit.

Regarding the setting u as a function of time t, we may let n increase indefinitely, and replacing τ by dt we obtain another representation of Eq. (1),

$$1/\sigma^2=P=\int\{[L'(u)]^2/L(u)\}dt, \tag{2}$$

which is somewhat more general than Eq. (1) since it holds regardless of how the interval is traversed. It should be reiterated that Eqs. (1) and (2) were based on the following approximations:

1. All counting intervals contain enough counts so that the Poisson distribution may be approximated by a normal distribution.

2. All errors are small enough so that, within their range, the curve $L(u)$ does not change slope appreciably.

Of these two approximations the second one is the more serious since it tends to break down when one considers extremely weak lines. Nevertheless, this assumption is necessary for a systematic analysis of these errors.

In order to obtain an explicit expression for the errors in fitting a particular profile we make the following additional approximations:

3. Points on the profile are uniformly spaced and sufficiently closely spaced that a continuous distribution of points may be used to approximate the actual discrete distribution.

4. The line profile has the shape of an isosceles triangle, its apex representing the line peak, and the extended background representing its base.

This simple profile seems to be very nearly the shape of the actual one in many cases (see Fig. 9) and certainly is not so far wrong as to cause a greatly incorrect estimate of P.

Assigning a base width W to the line and a peak height H above background B, we obtain $[L'(u)]^2=4H^2/W^2$ over the profile so that if a total time T is required to cross the line, then

$$P=\frac{2T}{W}\int_0^{W/2}\frac{4H^2/W^2}{(2Hl/W)+B}dl,$$

giving

$$P=1/\sigma^2=(4HT/W^2)\log[(H+B)/B]. \tag{3}$$

Actual lines which have been investigated have σ's as calculated by Eq. (3) which are less than 0.001 milliangstrom in almost all cases, and for this reason we feel that errors due to random variations in counting rate are considerably smaller than instrumental errors.

[8] This analysis only aims to give that component of the total error in the wavelength determination which comes from one cause alone, the statistical fluctuations of counting.

[9] In actual practice the composite profile is fitted to the observed points on the profile of a given line, not by the laborious numerical method of least squares, but by a visual estimate of the "best" fitting position. It is found by actual test that this can be judged with remarkable accuracy in accord with the least squares criterion. Hence for this analysis a least squares fit is assumed. Errors resulting from imperfect visual fitting of the composite profile have been studied and have been found experimentally to be of the same order or less than those due to statistical fluctuations of counting.

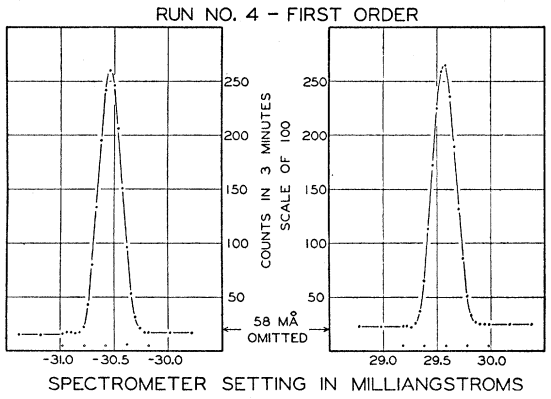

FIG. 9. A typical pair of line profiles. This pair of profiles was obtained for the 412-kev gamma-radiation following decay of gold 198. The wavelength is found by first forming a composite profile by superposition of all profiles (plotted to the same scale) obtained with the same source and then matching each profile individually to the composite profile. The difference in screw readings for the two members of a pair corresponding to a fiducial mark on the composite profile gives twice the wavelength, before corrections.

III. IRIDIUM 192

Iridium 192 has been found to decay with a half-life of 70 days by both β^- emission and K capture.[10] The end point of the β^- spectrum as measured by Mandeville and Scherb and others[11–13] corresponds to an energy of about 0.6 Mev, the exact end point being difficult to measure because it is obscured by internal conversion lines. A simple spectrum is thought to exist, however, since the ratio of beta-gamma coincidence counting rate to β-counting rate does not seem to vary as β-absorber is placed in front of the β-counter. Mandeville and Scherb have also found by means of coincidence measurements that each β-ray is followed on the average by 0.6 Mev of gamma-radiation.

We infer from the presence of osmium K x-rays, along with those from iridium and platinum, in the spectrum from a neutron activated source of iridium 192 that iridium 192 also decays by the process of K capture to osmium 192 with the possible emission of gamma-rays following this decay. K capture leaves the atom of osmium ionized in the K shell, thus giving rise to K x-rays. Cork[10] has confirmed this conclusion by detecting Auger electrons corresponding to osmium x-rays.

A list of our measured x-ray lines from a neutron-activated source of iridium 192 is given in Table III, where present measurements of wavelengths are compared with those of Ingelstam.[14] Intensities of the K spectra of osmium, iridium, and platinium were observed to lie in the ratio 1:1.7:1.3. While K lines of iridium are, no doubt, excited by fluorescent absorption of gamma-rays in the source material, those of platinium must be produced by internal conversion of the gamma-rays following β^- decay. Since the needed internal conversion coefficients are not known, it is not possible to determine quantitatively, from a comparison of x-ray intensities, the relative probabilities of K capture and β^- decay. On the other hand, we can be certain that the latter has the greater probability, since osmium x-rays are the least intense of all.

By studying characteristics of the peaks obtained during the search for lines from iridium 192, it is possible to make an interpretation of them in terms of gamma-rays and x-rays appearing in the first, second, and third orders of reflection from the quartz crystal.

X-ray lines may be identified in a number of ways. In the first place, their wavelengths are fairly well known so that by accurate measurement alone a positive identification can be made. Second, the natural breadths of the K lines are quite comparable to instrumental breadths of the spectrometer so that they appear detectably broader than gamma-lines, whose natural breadth is quite negligible. Finally, the x-ray lines appear in characteristic series having definite intensity ratios, so that a complete series may be expected and the positions of the lines predicted in advance.

Second and third orders of intense gamma- and x-ray lines appear at spectrometer settings corresponding to two and three times the wavelength of the first-order reflections. Intensities of first- to second- to third-order reflections were found to lie in the ratio 1:0.013:0.005 [quartz (310) planes]. Identification of the various orders was thus achieved by comparing spectrometer settings and intensities. A positive identification could also be made in all cases by use of the scintillation counter as a low resolution spectrometer operating in tandem with the crystal diffraction spectrometer to separate orders of reflections. Gamma- and x-ray lines will thus produce scintillation pulse-height spectra corresponding to the energy of the reflected photons and independent of the order of reflection. Using the

TABLE III. Wavelengths (in milliangstroms) of x-rays which follow decay of iridium 192.

Designation	Present measurement	Measurement by Ingelstam
Os $K\alpha_2$	201.620	201.627
Os $K\alpha_1$	196.771	196.783
Ir $K\alpha_2$	195.869	195.889
Ir $K\alpha_1$	191.031	191.033
Pt $K\alpha_2$	190.362	190.372
Pt $K\alpha_1$	185.485	185.504
Os $K\beta_3$	174.418	174.424
Os $K\beta_1$	173.584	173.607
Ir $K\beta_3$	168.524	168.533
Pt $K\beta_3$	164.463	164.489
Ir $K\beta_2^{II}$	164.009	164.139
Ir $K\beta_2^{I}$		163.944
Pt $K\beta_1$	163.661	163.664
Pt $K\beta_2^{II}$	159.257	159.374
Pt $K\beta_2^{I}$		159.184

[10] Cork, LeBlanc, Stoddard, Childs, Branyan, and Martin, Phys. Rev. **82**, 258 (1951).
[11] C. E. Mandeville and M. V. Scherb, Phys. Rev. **73**, 1434 (1948).
[12] L. J. Goodman and M. L. Pool, Phys. Rev. **71**, 288 (1947).
[13] P. W. Levy, Phys. Rev. **72**, 352 (1947).
[14] E. Ingelstam, Nova Acta Regiae Soc. Sci. Upsaliensis **73**, 812 (1948).

above methods, it was possible to pick out from the 38 peaks originally noted, 11 distinct nuclear gamma-rays lying between the energies of 136.33 kev and 612.87 kev. Of these eleven, the four gamma-rays having energies of 467.98 kev, 316.46 kev, 308.45 kev, and 295.94 kev were five to ten times as intense as any other lines present and were all obtained in the second and third orders as well as in the first order. Four much weaker lines of higher energy were also measured at energies of 484.75 kev, 588.40 kev, 604.53 kev, and 612.87 kev, the last pair comprising a fairly close doublet which had to be separated by use of a composite profile.

A complete list of gamma-ray wavelengths and energies, together with their approximate intensities and estimated errors is given in Table IV, while a comparison of these measurements with results previously obtained by use of beta-ray spectrometers is given in Table V. For the sake of consistency, only first-order measurements are listed in these tables.

TABLE IV. Wavelengths and quantum energies of gamma-rays following decay of iridium 192.

Identification letter[a]	Wavelength in milliangstroms	Energy in kev	Relative intensity[c]
A	20.227±0.020[b]	612.87 ±0.61	50
B	20.506±0.020[b]	604.53 ±0.59	140
C	21.068±0.010	588.40 ±0.28	110
	25.573±0.010	484.75 ±0.19	110
D	26.489±0.004	467.984±0.061	3000
E	39.172±0.004	316.462±0.034	9900
F	40.189±0.004	308.454±0.033	3700
G	41.888±0.004	295.942±0.031	3800
	60.254±0.011	205.736±0.038	750
	61.580±0.011	201.306±0.037	100
H	90.929±0.012	136.331±0.019	40

[a] Only those lines which can be assigned to platinum 192 have been given identification letters. This identification was made by Cork and his co-workers from β-ray spectrometer studies.
[b] Errors in these two measurements are greater because the line profiles overlapped and had to be separated by using the composite profile.
[c] Relative intensities of lines having greatly different energies cannot be compared reliably because the variation of sensitivity of the spectrometer with energy is not accurately known for this source.

TABLE V. A comparison of present measurements with various other determinations of gamma-ray energies in kev from iridium 192.

Present measurement	Cork *et al.*[a]	H. & M.[b]	Levy[c]	Cork[d]	Deutsch[e]
				651	
612.87	611.2		615	610	
604.53	603.7		607	601	603
588.40	588.6		591	586	
484.75	484		488	477	
467.98	467.4		468	466	467
	415.1				
316.46	316.1	317	316	315	
308.45	307.7	308	307	306	307
295.94	294.9	296	295	294	
	283			269	
205.74	205.7	208	209		
201.31	201.1				
136.33	135.9	137			

[a] See reference 10.
[b] R. D. Hill and W. E. Meyerhof, Phys. Rev. **73**, 812 (1948).
[c] See reference 13.
[d] J. M. Cork, Phys. Rev. **72**, 581 (1947).
[e] M. Deutsch, Phys. Rev. **64**, 265 (1943).

A level scheme involving all but the four gamma-lines at 201.31 kev, 205.74 kev, 484.75 kev, and 588.40 kev may be constructed as shown in Fig. 10, in which different Ritz combinations of the various lines agree in energy to better than their estimated errors. This scheme is also in good agreement with observed intensities and is essentially the same as the one proposed by Cork in 1951.[10] Its construction was permitted by the use of the following energy combinations:

$$\begin{aligned} &295.94 \text{ kev}+308.45 \text{ kev}=604.53 \text{ kev};\\ &136.33 \text{ kev}+467.98 \text{ kev}=604.53 \text{ kev};\\ &295.94 \text{ kev}+316.46 \text{ kev}=612.87 \text{ kev}. \end{aligned} \qquad (4)$$

Gamma-ray energies combine with such exactness (well within their assigned errors, given in Table IV) that the validity of these combinations seems practically certain. The level scheme of Fig. 10 which was derived from these combinations is, however, by no means unique, since by permuting the orders of the various lines within the combinations, it is possible to arrive at other level schemes. Level schemes obtained in this way, such as the one in Fig. 11, involve the same combinations, but are otherwise quite different. The level scheme of Fig. 11 has the advantage over the first level scheme of agreeing with the assertion of Mandeville and Scherb that 0.6 Mev of gamma-radiation follows beta-emission, but the disadvantage not present in the first scheme of disagreeing decidedly with the intensity ratios noted during the present measurements.[15]

Topological Method of Enumerating Level Schemes

Since various energy level schemes may be constructed from a given set of Ritz combinations, it is of interest to see how many ways a given set of combina-

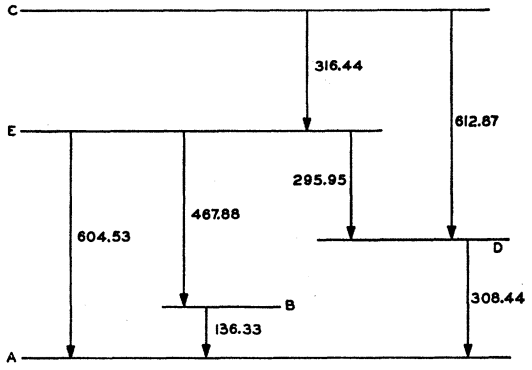

FIG. 10. Proposed energy level scheme for platinum 192.

[15] Intensities of the lines at 295.94 kev and 308.45 kev are about the same, while the intensity of the one at 316.46 kev is more than twice this. In the scheme of Fig. 11, one would expect the intensity of the 295.94 kev line to be greater than the sum of the other two.

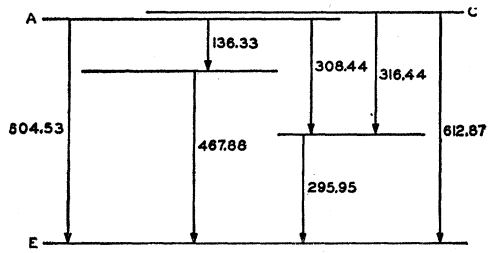

FIG. 11. Alternate energy level scheme for platinum 192.

tions may be permuted to give different level schemes, and to attempt to devise a system for enumerating these schemes quickly and easily. Physical considerations such as intensity ratios, coincidence studies, multiplicity of β-rays, and multipolarity of gamma-radiation provide the basis for determining the most likely of the several permutations.

In a general scheme consisting of N levels, L gamma-lines, and C algebraically independent Ritz combinations, let us concentrate on a particular combination such as one of Eqs. (4). Taking an arbitrary line of this combination, we discover that the level from which it originates has one, and only one other line of the combination, either passing to it or away from it. This line in turn passes either away from, or to another level where a third line of the combination has its terminus, so we may pass in a circuit around the various lines of the combination until we arrive at the original line where we started. Such a circuit may be represented graphically on a topological diagram as a loop with the various levels appearing as dots or points and the gamma-lines as the connecting lines between these points. Other combinations, involving perhaps some of the same gamma-rays, form other circuits containing points (or levels) and lines in common with this one and the whole is thus represented as a network. In this topological network the lengths of the various lines in no way correspond to gamma-ray energies, and consequently this representation conveys no numerical information concerning the combinations, but instead may be used to show at a glance their topology. The topological network representation of the iridium level scheme is shown in the upper drawing of Fig. 12.

Given such a network, it is possible to construct the associated decay scheme if one knows the line energies and the signs to be attached to these energies in each circuit.[16]

Once the network representation for a level scheme has been obtained, it is possible to arrive at other level schemes having the same independent combinations (or circuits) by permuting the orders of lines appearing in the various circuits in such a way as to avoid changing the lines appearing in any circuit. In the lower drawing of Fig. 12, lines a and b have been interchanged, thus changing the level scheme from the one appearing in Fig. 10, represented by the upper drawing of Fig. 12, to the one appearing in Fig. 11. Clearly, still other level schemes could be constructed by interchanging c and d or by interchanging both c and d, and a and b. Still more schemes may be constructed by inverting the orders of all lines in all the circuits thus effecting a mirror transformation. This type of transformation corresponds to turning the entire level scheme upside down, and is always possible, even when no other permutations are permitted. By considering all possible permutations of the scheme in Fig. 12, eight different networks of this type having the circuits of the original scheme, may be constructed. Two of these additional schemes may be obtained by inverting those of Figs. 10 and 11, while the remaining four result from the interchange of the 467.98-kev and the 136.33-kev lines. An inspection of any network of this type will disclose which permutations of lines may be made without destroying the existing circuits and the resulting level schemes may be constructed.

[16] A positive sign may be arbitrarily attached to a line in a combination if, as one passes around a circuit, one goes from the final to the initial state, while a negative sign may be attached if one goes from the initial to the final. The algebraic sums of the lines contained in any circuit is therefore zero.

IV. TANTALUM 182

The radiations from tantalum 182 and its daughter tungsten 182 have been studied by several groups.[17–24] With the single exception of reference 20, where absorption and coincidence methods were used, all of these investigations were made with β-ray spectrometers. In reference 23 Beach, Peacock, and Wilkinson reported the presence of at least one group of beta-particles (with end point at 0.525 Mev), 3 intense gamma-rays in the neighborhood of 1.2 Mev, and 17 low energy gamma-rays (<0.33 Mev). The most recent paper[24] by the Michigan group gives 14 to 18 low energy gamma-rays; this same paper proposes a nuclear energy level scheme of 8 levels to account for these gamma-ray lines. No attempt was made to fit the 3 high energy lines into this scheme.

The great number of gamma-ray lines produced in the decay of tantalum 182 has made it difficult to construct nuclear energy level schemes with certainty, especially in view of the limited accuracy of the beta-ray spectrometers used. This isotope was therefore selected for a precision investigation using the curved crystal gamma-ray spectrometer. This investigation has been carried out during the past two years. A total of 16 gamma-ray lines was detected and measured. These lines can be fitted together into several tentative energy level schemes.

[17] Zumstein, Kurbatov, and Pool, Phys. Rev. **63**, 59 (1943).
[18] W. Rall and R. G. Wilkinson, Phys. Rev. **71**, 321 (1947).
[19] J. M. Cork, Phys. Rev. **72**, 581 (1947).
[20] C. E. Mandeville and M. V. Scherb, Phys. Rev. **73**, 340 (1948).
[21] Cork, Keller, Sazynski, Rutledge, and Stoddard, Phys. Rev. **75**, 1778 (1949).
[22] C. H. Goddard and C. S. Cook, Phys. Rev. **76**, 1419 (1949).
[23] Beach, Peacock, and Wilkinson, Phys. Rev. **76**, 1585 (1949).
[24] Cork, Keller, Rutledge, and Stoddard, Phys. Rev. **78**, 95 (1950).

Two different sources of neutron irradiated tantalum were used during the investigations. Only the results obtained with the second of these sources are reported here, since we feel that these are the more reliable. With this source 18 gamma-rays were detected in the preliminary search runs. In addition, the $K\alpha_1$, α_2, β_1, β_3, and β_2 x-rays of tungsten and the $K\alpha_1$, α_2, β_1, and β_3 x-rays of tantalum were detected. The x-rays of hafnium were not detected; thus there is no evidence for K capture in tantalum 182. The detection of the W $K\alpha_1$ x-ray line permitted the instrument to be calibrated without the installation of the heavy x-ray tube and its stiff high voltage cables, which could easily produce mechanical flexures in the spectrometer. Such a calibration was performed both before and after the gamma-ray measurements. This method of calibration was used in connection with all of the measurements reported in this paper.

Satisfactory measurements were obtained for 16 of the gamma-ray lines. The final results are presented in Table VI. One of the remaining two lines, at about 108 kev, was so weak that it could not be detected sufficiently well for a good measurement. The other line, at about 250 kev, appeared as a strong line during two different search runs, but decayed below the minimum intensity for measurement during the one month interval between the searches and the measurements. This is definitely contrary to the known half-life of 112 days of tantalum 182. Since the two searches in which the line was detected were about a week apart and on opposite sides of the instrument, it is difficult to explain this effect by a freakish behavior of the spectrometer.

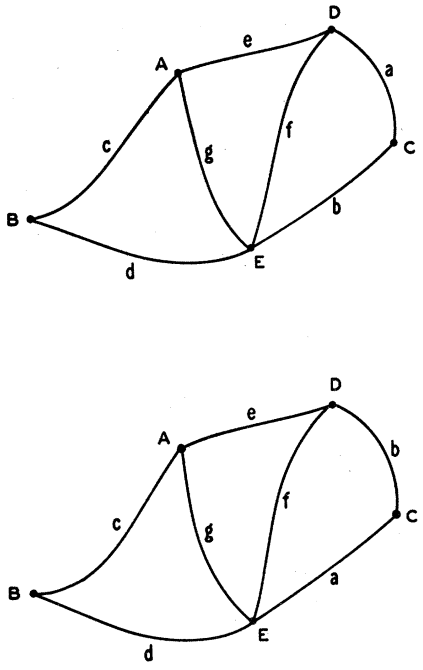

FIG. 12. Topological representation of the energy level schemes of Figs. 10 (above) and 11 (below).

TABLE VI. Wavelengths, energies, and relative intensities[a] of gamma-radiation following decay of tantalum 182. The uncertainties given are standard deviations.

Identification letter	Wavelength in milliangstroms	Energy in kev	Relative intensity[a]
A	10.134±0.010	1223.25±1.21	334
B	10.437±0.015	1187.74±1.70	157
C	11.057±0.010	1121.14±1.02	352
D	46.941±0.011	264.086±0.060	27
E	54.070±0.011	229.266±0.046	24
F	55.827±0.011	222.051±0.044	45
G	62.512±0.011	198.305±0.036	9
H	69.115±0.011	179.360±0.030	19
I	79.277±0.012	156.369±0.024	14
J	81.337±0.012	152.408±0.023	43
K	106.500±0.013	116.398±0.014	2
L	109.071±0.013	113.655±0.014	9
M	123.851±0.014	100.092±0.012	46
N	146.414±0.015	84.667±0.009	6
O	183.010±0.018	67.736±0.007	100
P	188.643±0.018	65.714±0.006	9

[a] All factors except internal conversion have been taken into account in calculating the relative intensities.

We have not been able to identify the line with any *known* impurity in the source sample. A comparison with the adjacent 264-kev line in the two search runs indicates a half-life of about 7–10 days for the 250-kev line. We plan to investigate this effect with a new source of tantalum 182 in the near future.

Since the measurements of the 16 gamma-ray lines of Table VI were made prior to the new calibration reported above, it was necessary to use a calibration curve to correct for the mirror correction. The hysteresis effects known to be present cannot be included in such a curve, and hence the measurements might be more in error than is indicated by the consistency of successive measurements. Consequently, the arbitrary value of 0.010 screw division was assigned as the error. This value is believed to be large enough to account for errors due to hysteresis. In the case of the line designated by the letter *B*, the source was so wide that although the line could be resolved from the adjacent line *A* with the aid of the composite profile, the accuracy of the determination was seriously impaired. Therefore, the following procedure was adopted: The wavelength of line *A* was determined from the data obtained with the second source; then the difference, $\lambda_B - \lambda_A$, determined with the first source, was added to the wavelength of line *A* to get the wavelength of line *B*. The first source was about one-third as wide as the second source; consequently the lines were clearly resolved for this source, since the resolution of the spectrometer was much better. The value obtained in this manner is believed to be more reliable; however, a larger error (0.015 screw division) has been assigned to this line. The errors were assigned before conversion to milliangstroms; consequently, the errors given in Table VI are somewhat larger, since there also is an error associated with the factor for converting from screw divisions to milliangstroms.

TABLE VII. Equations[a] for determining the energy level scheme for tungsten 182.

I	II	III Discrepancy: column I − column II in kev[b]	IV Standard deviation in kev	V Identification number
$G+P=D$		−0.067	0.070	(1)
$I+P=F$		−0.059	0.068	(2)
$L+N=G$		+0.017	0.039	(3)
$L+P=H$		+0.009	0.034	(4)
$N+O=J$		−0.005	0.025	(5)
$C+O=B$		+1.14	1.99	(6)
$M+C=A$		−2.02	1.58	(7)
$A+G=B+E$		+4.55	2.09	(8)
$A+K=B+I$		−4.46	2.09	(9)
$A+K=B+J$		−0.50	2.09	(10)
$A+E=B+D$		+0.69	2.09	(11)
$A+L=B+J$		−3.24	2.09	(12)
$A+N=B+K$		+3.78	2.09	(13)
$A+M=C+G$		+3.90	1.58	(14)
$B+J=C+F$		−3.04	1.99	(15)
$B+K=C+H$		−3.64	1.99	(16)
$C+P=B$		−0.89	1.99	(17)

[a] Only independent equations are listed here.
[b] Equations containing two of lines A, B, and C have been rejected if the discrepancy was over 5 kev. Equations not containing any of the lines A, B, and C have been rejected if the discrepancy was more than 5 times the standard deviation.

Energy values and relative intensities are also given in Table VI. The energies were found from the wavelengths by using the conversion factor 12396.44±0.25 kev-milliangstroms.[25] To determine the relative intensities, the observed intensities (measured by the heights of the peaks above background) were corrected for (1) the reflection coefficient of the crystal, which is proportional to λ^2, (2) self-absorption in the source, and (3) counter efficiency, which is assumed to depend only on the absorption of the gamma-ray beam in traversing the 1-inch thickness of the scintillation crystal. Internal conversion could not be taken into account because neither the nature of the radiation nor the internal conversion coefficients (for the lower energies) are known.

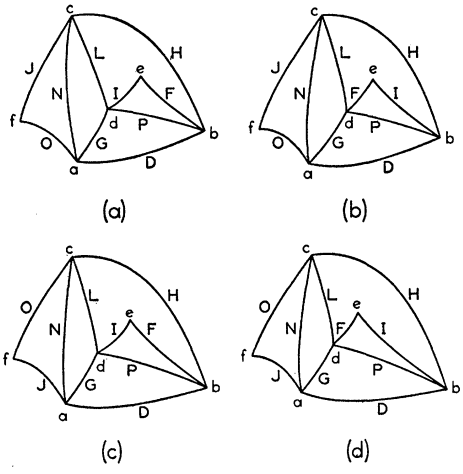

FIG. 13. Topological maps representing four possible energy level schemes for ten gamma-ray lines from tungsten 182. The lines are identified by the upper case letters assigned to them in Table VI. Lower case letters at the intersections represent energy levels. The four permutations are obtained by interchanging lines F and I and lines J and O as indicated. The corresponding energy level schemes are given in Fig. 14.

[25] J. W. M. DuMond and E. R. Cohen, Report to the National Research Council Committee on Constants and Conversion Factors of Physics, December, 1950; Phys. Rev. 82, 555 (1951).

The topological method for determining and enumerating level schemes described above was also used in an attempt to find a level scheme for tungsten 182. From all possible sums and differences of two gamma-ray energies, the equations of Table VII were selected for possible use in determining level schemes. The

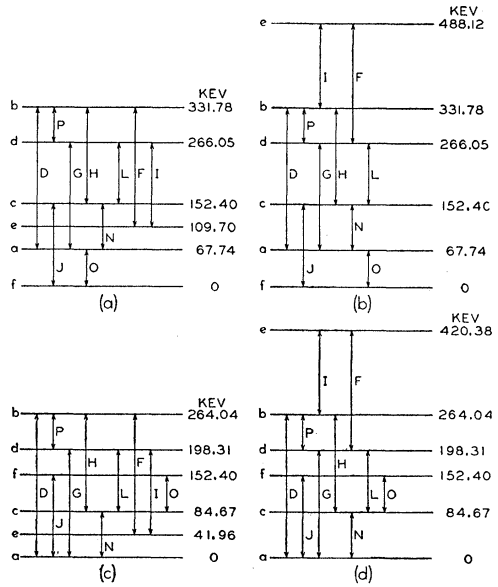

FIG. 14. Four possible energy level schemes for ten gamma-ray lines from tungsten 182. These schemes correspond to the four topological maps of Fig. 13 and are designated in the same manner. The lowest level has been arbitrarily assigned the value zero. An additional four possible level schemes can be found by inverting the four schemes shown here. One of these eight level schemes for these ten gamma-ray lines should, we believe, be incorporated into the final level scheme for tungsten 182 when it is determined.

criteria used in selecting these equations were as follows: (1) only independent equations were to be listed; (2) equations containing the lines A, B, and C, which have large errors, could not have a discrepancy over 5 kev; (3) equations not containing any of the lines A, B, and C could not have discrepancies greater than 5 times the corresponding standard deviations. Clearly it will be impossible to use all of these equations in formulating a level scheme, since some are incompatible with others. Undoubtedly some of the equations are accidental, and these must be determined by trial and error and rejected. The first five equations of Table VII were chosen as a starting nucleus, since none of them has a discrepancy of more than 100 electron-volts. Furthermore, the discrepancies for these equations are all

less than the corresponding standard deviations. The resulting topological maps for the 10 gamma-ray lines contained in these 5 equations are shown in Fig. 13. There are 4 possibilities to be considered, since lines F and I or lines J and O may be interchanged without affecting the equations from which the maps are constructed. The energy level schemes corresponding to these maps are shown in Fig. 14. Four additional level schemes can be obtained by inversion of those given in the figure, since the choice of the ground state is (so far) arbitrary. The schemes presented in Figs. 13 and 14 have been determined solely on the basis of the Ritz combinations given in the first 5 equations of Table VII. It is impossible to choose between the 8 possibilities represented here without the use of additional equations and other information such as relative intensities, known β-rays associated with the decay process, internal conversion coefficients, etc.

Attempts to extent the level schemes by including more lines, for the most part, have not been very satisfactory. Using only the 16 lines which we have measured, it seems impossible to obtain a level scheme containing all of these lines. This is not unreasonable, since there are undoubtedly a number of lines which we have not been able to detect with the gamma-ray spectrometer, and these lines could conceivably be just those needed to complete the level scheme. We have succeeded in obtaining several topological maps containing 14 or 15 of the measured lines, each of which has 24 or more permutations. Eliminations of these different maps must be made on the basis of relative intensities, known beta-rays, internal conversion coefficients, etc., and the unsatisfactory nature of this information to date makes such eliminations difficult. Furthermore, our results for the high energy lines A, B, and C are not sufficiently accurate to enable one to choose the proper equations from the large number in Table VII which contain these lines. For these reasons we have been unable to formulate with reasonable certainty any level scheme which contains the three high energy lines. The maps for two of perhaps half a dozen different possibilities are given in Fig. 15. Until more, and more accurate, information is available, it seems unlikely that the actual level scheme can be determined. A program for future work on tantalum 182 at this laboratory has been outlined, and we plan to begin work in the very near future. Use of the gamma-ray spectrometer in conjunction with the axial focusing homogeneous magnetic field β-ray spectrometer,[26] the construction of which was completed only recently, is expected to provide the additional information necessary for the completion of the level scheme.

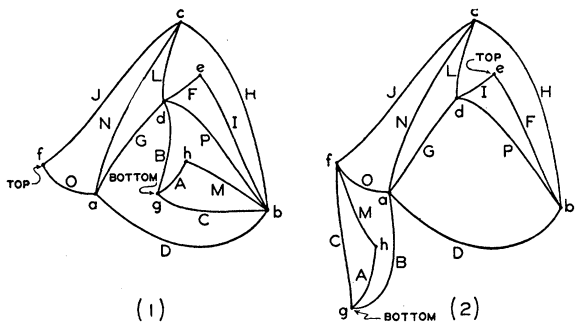

FIG. 15. Topological maps for two possible energy level schemes for 14 gamma-ray lines from tungsten 182. These two maps clearly point out the need for greater precision in the 1-Mev region, since on the basis of present accuracy and the present state of additional information on beta-ray spectra and internal conversion one cannot decide between Eqs. (6) and (17) of Table VII. These two equations give the two topological maps shown here. Several other possible energy level schemes for 14 or 15 gamma-ray lines can also be obtained from the information now available.

TABLE VIII. Energies and intensities of gamma-rays of the thorium series.

Line energy as measured by other investigators, in kev	Present observed energy in kev, and standard error	Present observed intensity
	ThB—ThC transition	
238.61±0.08[a]	238.595±0.032	1
	ThC—ThC′ transition	
726[b]	729.3±1.7	0.15
	ThC″—ThD transition	
276.5[b]	277.350±0.063	0.05
510.90±0.09[a]	510.75 ±0.15	0.15
582.3[b]	582.978±0.27	0.4
	Unassigned	
	240.984±0.033	0.1

[a] See reference 29.
[b] See reference 28.

V. NATURAL THORIUM SERIES

A 150-millicurie sample of radiothorium[27] was used for the measurement of certain lines of ThC, ThC′, and ThD. The results of these measurements are tabulated in Table VIII. The relative intensities of the lines have been estimated by correcting for the change in sensitivity of the scintillation counter with wavelength (assumed equal to the change in absorption of the scintillating crystal), the self-absorption of the source and its platinum-iridium capsule, and the change in reflecting power of the crystal. The tabulated error has been evaluated by combining the standard deviation given by the consistency (reproducibility) of the instrument in repeating observations of a given gamma-ray line with the errors associated with the calibration and conversion factors. These gamma-ray lines have been measured by other investigators[28–30] and the most precise of their results, expressed in terms of quantum energy, have been included in the table for comparison.

[26] DuMond, Bogart, Kohl, Muller, and Wilts, Special Technical Report No. 16, California Institute of Technology, March, 1952 (unpublished).
[27] We are indebted to R. B. Holt and N. F. Ramsey of the Radiation Laboratory, Harvard University, for the generous loan of this source.
[28] See Rutherford, Chadwick, and Ellis, *Radiations from Radioactive Substances* (Cambridge University Press, Cambridge, 1930).
[29] G. Lindstrom, Phys. Rev. 83, 465 (1951).
[30] H. Craig, Phys. Rev. 85, 688 (1952).

TABLE IX. Energies and intensities of gamma-rays of the radium series.

Ellis *et al.* energy, kev	Present observed energy in kev, together with standard error	Present observed relative intensity
	RaB−RaC transition	
52.9	53.226±0.0014	
240.6	241.924±0.030	0.2
293.7	295.217±0.039	0.55
349.9	351.992±0.062	1
	RaC−RaC′ transition	
606.7	609.37±0.16	1.6
	Po $K\alpha_1$ x-ray line	
	79.290±0.015	

For this purpose the data of Lindstrom (expressed as electron momentum in gauss-cm) have been converted to electron kinetic energy in electron kilovolts through the use of the latest values of the atomic constants and conversion factors.[25] To these quantum energies were added appropriate binding energies through the use of the values of the Bi L_{I} and Pb K absorption edges published by Cauchois and Hulubei,[31] as well as the value of E_K-_{LI} for Bi given by Cauchois.[31] The limits of error correspond to estimated probable error given by Lindstrom. The present results agree with those of Lindstrom well within the experimental error. This agreement was not encountered with our older results.

Many other lines have been reported but careful search has shown them to be too weak to measure with the present instrument. The source was not of optimum shape for the curved crystal spectrometer, being a cylinder 2 mm in diameter and 4 mm long encased in a capsule 0.5 mm thick. This resulted in a large background contribution and a weak beam, since it was necessary to mask the source in order to obtain resolution. Carefully designed masking jaws were used but with no success in detecting the 2.6-Mev gamma-ray of ThD.

The observed line of energy 240.98 kev has not been identified. It is close to the 241.92-kev line of RaC but the difference between them far exceeds the limits of error. Since this line is only one-tenth as strong as the 238.59-kev line of ThC and only one percent different in energy, the β-ray spectrometers may have failed to resolve it.

VI. RADIUM C AND RADIUM C′

The gamma-ray spectrum of the radium series was studied by the use of the emanation radon. Several sources of approximately 100-millicurie strength were employed,[32] and it was possible to make measurements even after the source had decayed to 8 millicuries.

[31] Y. Cauchois and H. Hulubei, *Longeurs d'Onde des Emissions X* (Herman & Cie, Paris, 1947).

[32] We are greatly indebted to Dr. C. Emery and Dr. G. L. Locher of the Emery Tumor Group, Los Angeles, and Western Radiation Laboratories, Los Angeles, for making these Rn samples available to us.

The results of measurement of four lines of RaC and of one line of RaC′ are given in Table IX. The uncertainties are standard errors based on consistency of repeated observations, since the error due to all unknown systematic errors is thought to be small. Three or four measurements were made on each of these lines and the results averaged. The standard error of a single measurement was obtained by the usual formula,[33]

$$\sigma_{x_s}=\{[\Sigma(\delta x_i)^2]/(n-1)\}^{\frac{1}{2}}, \tag{5}$$

for each of the gamma-ray lines. Since it is felt that the uncertainty in wavelength of a single observation is independent of wavelength, the weighted rms value of these deviations σ_{x_s} was determined. The standard error of the determination of wavelength of a line was taken to be this value divided by $\sqrt{n}$ where n is the number of observations, in accord with the usual expression for the standard error of the mean of n observations,

$$\sigma_{x_m}=\{[\Sigma(\delta x_i)^2]/[n(n-1)]\}^{\frac{1}{2}}. \tag{6}$$

In the energy determinations, the uncertainty of knowledge of the W $K\alpha_1$ calibrating line introduced additional error. This completely masked the above-mentioned internal consistency uncertainty in the case of the 52-kev line, and had a slight effect on some of the others.

The estimated relative intensities were determined by correcting for the efficiency of the scintillation detector, for the reflection coefficient of the crystal, and for decay of the source between measurements. Uncertainty of the counter sensitivity at 52 kev prevented a comparison of its intensity with the other lines.

A single close relation was expected to occur between the 52-kev line, the 242-kev line, and the 295-kev line. It runs as follows:

$$(241.924\pm0.030)+(53.226\pm0.0014)-(295.217\pm0.039)=0.067\pm0.049,$$

thus tending to verify the accepted decay scheme.[34]

The following x-rays were detected and identified: Bi $K\alpha_2$, $K\alpha_1$, $K\beta_3$, $K\beta_1$, $K\beta_2{}^{\mathrm{II}}$, and $K\beta_2{}^{\mathrm{I}}$. An additional x-ray line was measured and is believed to be the $K\alpha_1$ line of polonium. Its wavelength was obtained by measuring the difference between its wavelength and

TABLE X. Wavelengths and quantum energies of tungsten 187 γ-ray lines.

Wavelengths in milliangstroms	Energy in kev
18.069±0.010	686.06±0.38
20.030±0.010	618.89±0.31
25.852±0.010	479.52±0.19
92.341±0.012	134.25±0.018
172.174±0.017	72.00±0.007

[33] *Handbook of Chemistry and Physics* (Cleveland Chemical Rubber Publishing Company, Cleveland, 1944). See the explanation of the Mathematical Tables.

[34] M. Stern, Revs. Modern Phys. **21**, 316 (1949).

that of Bi $K\alpha_1$, listed in the tables.[31] The wavelength of the Po $K\alpha_1$ line is thus found to be 156.343±0.030 milliangstroms.

VII. TUNGSTEN 187

Results of the measurements of the five known gamma-rays of 24-hour tungsten 187 are in essential agreement with previous measurements[35–37] (see Table X).

The decay scheme of Beach, Peacock, and Wilkinson[35] appears to be correct in so far as the combination of 72.00 kev+134.25 kev+479.52 kev=686.06 kev checks well within instrumental errors, but the line at 618.89 kev does not combine with the 134.25-kev and 479.52-kev lines, as indicated in their decay scheme The corrected decay scheme for tungsten 187 shown in Fig. 16 does not include the 618.89-kev line, which apparently represents an independent transition.

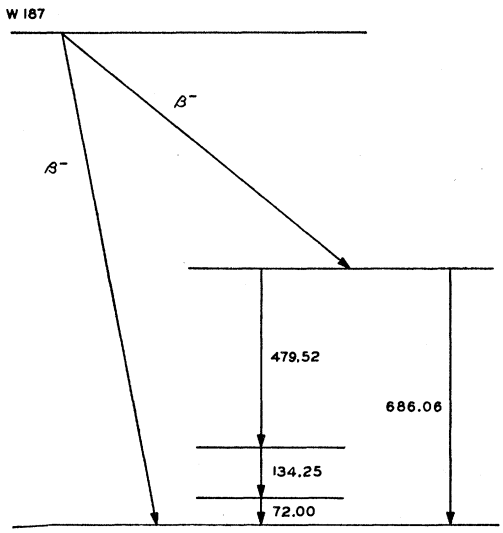

FIG. 16. Proposed decay scheme for tungsten 187.

VIII. CESIUM 137 AND GOLD 198

Measurements of the gamma-rays from cesium 137, gold 198, and the annihilation radiation from copper 64 were carried out after the calibration described above. Since the spectrometer was equipped with the 6-inch mirror at the time these measurements were made, it was possible to check the alignment of the long carriage with the crystal during the measurements. As a result, two to three times the precision otherwise attainable was possible.

The wavelength and energy of the single gamma-ray following decay of cesium 137 has been determined from the average of 6 measurements. The resultant values are $\lambda=18.737\pm0.004$ milliangstroms; $E=661.60\pm0.14$ kev.[38]

Several gamma-rays follow the decay of gold 198.[39–43] Of these, the strongest is the 412-kev gamma-ray line, which accompanies 99.7 percent of the decay processes. The fairly large neutron absorption cross section of gold 197 (96.4 barns), combined with this, makes it possible to obtain a source of sufficient activity to observe second- and third-order reflections for this gamma-ray line from our bent quartz crystal. It was hoped that, in addition to this, the high activity would be sufficient to permit measurement of one or more of the other lines from gold 198, as well as some of the gamma-ray lines following decay of gold 199, which is produced by neutron capture in gold 198.[44]

The source, a piece of 24-carat gold foil, was irradiated in the reactor at the Argonne National Laboratory, and had an activity of approximately 5 curies on arrival in Pasadena. Preliminary searches with the spectrometer showed that, as expected, the second- and third-order reflections of the 412-kev line could be detected; in addition, the 159-kev gamma-ray line following decay of gold 199 was found to be strong enough for a wavelength measurement. Unfortunately, however, it was necessary to confine all measurements to the 412-kev line.

A total of two runs in the third order, one run in the second order, and ten runs in the first order was made. Counting intervals were chosen so that one percent statistics or better were obtained at the peak of the profiles. A typical pair of profiles for the first order is shown in Fig. 9. To determine the composite profile, only the profiles obtained from the first-order runs were used. Decay corrections were not necessary, since only $2\frac{1}{2}$ hours or less was required to cross each line profile. The second- and third-order profiles were also matched to this composite, after decay corrections had been made.[45]

The final results of the experiment are given in Table XI. The average of the wavelengths (in screw divisions) obtained in each order are listed separately.

[35] Beach, Peacock, and Wilkinson, Phys. Rev. **75**, 211 (1949).
[36] C. L. Peacock and R. G. Wilkinson, Phys. Rev. **74**, 601 (1948).
[37] Hole, Benes, and Hedgran, Arkiv. Mat. Astron. Fysik. **35A**, No. 35 (1948).
[38] We are much indebted to A. F. Rupp of Oak Ridge for preparation of a suitable source of cesium 137.
[39] R. W. Pringle and S. Standil, Phys. Rev. **80**, 762 (1950).
[40] L. G. Elliott and J. L. Wolfson, Phys. Rev. **82**, 333 (1951).
[41] Bross, Ketelle, Zeldes, and Fairstein, Phys. Rev. **84**, 586 (1951).
[42] Cavanagh, Turner, Booker, and Dunster, Proc. Phys. Soc. (London) **A64**, 13 (1951).
[43] Patrick E. Cavanagh, Phys. Rev. **82**, 791 (1951).
[44] P. M. Sherk and R. D. Hill, Phys. Rev. **83**, 1097 (1951).

[45] The half-life of gold 198 has been determined by L. M. Silver, Phys. Rev. **76**, 589 (1949). The half-life of gold 198 was also calculated from the data for the first-order reflections. To do this, the height of the profile peak above background and the corresponding time at which the peak was reached were used. The values were obtained by using a least squares process to find the slope of the straight line representing the decay function when plotted in its logarithmic form. Because of a slight asymmetry in the profiles obtained on opposite sides of the spectrometer (the heights are not equal), there are two separate sets of data to be analyzed. The average of the two values is

$$\tau_{\frac{1}{2}}=2.74\pm0.04 \text{ days.}$$

This agrees with Silver's value of 2.69±0.015 days.

TABLE XI. The wavelength and energy of the 412-kev gamma-ray line following decay of gold 198, as obtained by measurements of first-, second-, and third-order reflections. The uncertainties given are standard deviations; these are given to one extra place to avoid incorrect weighting when combining these values with those of other experimenters.

Order	Wavelength in screw divisions	Wavelength in milliangstroms	Energy in kev
1	30.016±0.0028		
2	30.019±0.0023		
3	30.021±0.0016		
Weighted mean	30.019±0.0012	30.105±0.0026	411.770±0.036

The final value is a weighted mean of these three values. This wavelength was used to calculate the energy of the gamma-ray line. The errors were determined by a careful analysis of the contributions of the calibration and correction factors, counting statistics, etc., to the total error of a measurement.

IX. THE ANNIHILATION RADIATION FROM COPPER 64

It is well known that positrons decay by the process of annihilation of positron-electron pairs. The energy released by the disappearance of the masses of the two particles appears as radiation. In most cases this radiation appears as two quanta, each having an energy of approximately 510 kev. One-quantum and three-quantum annihilation also take place, but the frequency of occurrence of such events is so low as to make a study of these effects impossible with the curved crystal spectrometer. Hence our studies have been limited to two-quantum annihilation.

If both positron and electron are at rest in the c.m. system of coordinates, the equivalence of mass and energy yields Eq. (7) below:

$$(m_+ + m_-)c^2 = 2h\nu = 2hc/\lambda_A. \quad (7)$$

In this relation m_+ and m_- are the rest masses of the positron and electron, respectively, c is the velocity of light, h is Planck's constant, ν is the frequency of the annihilation radiation, and λ_A is the wavelength. Rearranging (7), the wavelength is found to be

$$\lambda_A = 2h/(m_+ + m_-)c. \quad (8)$$

This is the wavelength in the c.m. system; in the lab coordinate system the observed wavelength will be altered by a Doppler shift due to the motion of the center of mass. However, there is no reason to assign a preferred direction to the motion of the center of mass; and therefore, when one considers all of the electron-positron pairs annihilating in a given time interval, the effect is a broadening of the observed line rather than a shift in the center of the line. If there should be a residual kinetic energy in the c.m. system, or if the potential energies of the two particles should not be equal in magnitude and opposite in sign, a shift in wavelength would result. It has been shown[46] that such effects, if present, are negligible. The observed wavelength then is that given by Eq. (8).

One of the principal problems in the measurement of the annihilation radiation wavelength with the curved crystal spectrometer is the source of positrons to be used. First, a fairly strong source of radiation is necessary; the radiation should correspond to an activity of 10 millicuries or better at all times. Second, only naturally radioactive or neutron-activated materials are economically feasible because of the source strength requirement. On this basis copper 64 was selected as the source material. Even with this most advantageous choice, however, additional difficulties are encountered. These follow: (1) copper 63 comprises only 69 percent of natural copper; (2) the neutron absorption cross section of copper 63 is relatively low—2.82 barns; (3) copper 64 has a short half-life for our purpose—12.8 hours; (4) copper 64 decays by three competing processes—K-capture, β^- emission, and β^+ emission—and positron emission occurs in only 17.5 percent of all cases; (5) as explained in greater detail in a previous paper,[46] the relatively long range of positrons before annihilation requires that the source be defined by a slit, thereby severely limiting the effective volume of the source. The steps taken to make the most of the available activity will be described in the following paragraphs.

Two problems must be considered in the design and construction of the slit jaws used to define the source: (1) The part of the source which the crystal "sees" must be limited by the slit; otherwise the source would appear to be rather large and diffuse because of the long range of the positrons before annihilation and the fact that the positrons are annihilated in the material surrounding the radioactive sample as well as in the sample itself. (2) Radiation penetrating the sides of the slit jaws causes the so-called source window to have "tails," which will also appear in the observed line profiles. From the discussion of the effect of counting statistics on the accuracy of measurement given above, it can be seen that the accuracy can be increased considerably by eliminating or minimizing these "tails," i.e., by causing the line profile to have the greatest possible steepness over the widest possible range of wavelength settings. The best solution to these two problems can be obtained by use of the design of Fig. 17 and by

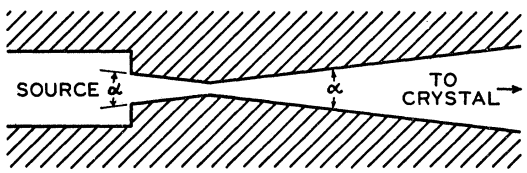

FIG. 17. Design for uranium slit jaws used to define Cu^{64} source in annihilation radiation experiment. $\alpha = 1.45°$. Width at narrowest point = 0.2 mm. Distance between source and narrowest point = 1 cm. The sketch is not to scale.

[46] DuMond, Lind, and Watson, Phys. Rev. 75, 1226 (1949).

making the slit jaws of a material having a very large absorption coefficient for the particular radiation which is to be studied. For the experiment reported here, uranium was chosen as the absorbing material. Sufficient uranium for the slit jaws was kindly made available to this project by the Atomic Energy Commission, and the slit jaws were made at the Brookhaven National Laboratory.

The source for the experiment was a rectangular block of copper, 0.080×0.497×1.25 in. This was irradiated at high neutron flux density in the reactor at the Argonne National Laboratory. Transportation to Pasadena was by special U. S. Navy plane. The activity of the source on arrival was approximately 7 curies; the useful activity (that is, that which resulted in annihilation radiation in the part of the source "seen" by the crystal) was equivalent to about 250 millicuries.

It had been hoped that the annihilation radiation line could be measured by second- and third-order reflection from the crystal planes, thereby increasing the precision of the measurements. However, preliminary calculations had shown that if the line were detected at all in these higher order reflections, it would be too weak to use successfully. Measurements immediately after installation of the source confirmed this. Consequently, all measurements were confined to the first-order reflections.

A 5-minute counting interval at each wavelength setting was chosen as a satisfactory value. This interval was kept fixed throughout the entire experiment. Thus all the profiles obtained were subject to the same distortion due to decay of the source. Since the important quantity is the difference in wavelength settings between corresponding points on the two members of a pair of profiles, the decay correction was not necessary for proper interpretation of the data. This eliminated possible errors due to additional arithmetic operations. Furthermore, the decay correction for the 3-hour interval required to cross a single profile is quite small. A total of nine pairs of profiles was obtained before the source had decayed below its useful limit. The results of the experiment are given in Tables XII and XIII.

TABLE XII. Illustration of the removal of the effect of hysteresis and the reproducibility of measurements. The values of 2λ (twice the wavelength), in screw divisions, for the annihilation radiation from copper 64 are given below. Comparison of the values before and after the mirror correction is applied indicates that the determination of the mirror correction for each run at the time of the experiment does indeed improve the reproducibility of the measurements.

Run No.	2λ Before mirror correction	2λ After mirror correction
1	48.328	48.383
2	48.352	48.390
3	48.338	48.388
4	48.320	48.381
5	48.332	48.385
6	48.328	48.378
7	48.326	48.384
8	48.336	48.390
9	48.344	48.392

TABLE XIII. Results on annihilation radiation. The uncertainties given after each ± are standard deviations. These are given to one extra place to avoid incorrect weighting when combining these values with those of other experimenters.

Wavelength:	
1. $\lambda_A=24.262\pm0.0033$ mA	Cu^{64} direct measurement of λ_A
2. $\lambda_A=24.263\pm0.0033$ mA	Au^{198} expt.+Hedgran and Lind
3. $\lambda_c=24.26067\pm0.00048$ mA	DuMond and Cohen least squares analysis
Energy:	
1. $E_A=510.941\pm0.067$ kev	Cu^{64} direct measurement of λ_A
2. $E_A=510.920\pm0.070$ kev	Au^{198} expt.+Hedgran and Lind
3. $m_-c^2=510.969\pm0.015$ kev	DuMond and Cohen least squares analysis
Positron mass:	
1. $(m_--m_+)/m_-=(1.01\pm1.85)\times10^{-4}$	Cu^{64} direct measurement of λ_A
2. $(m_--m_+)/m_-=(1.92\pm2.80)\times10^{-4}$	Au^{198} expt.+Hedgran and Lind

Table XII illustrates the slight variation in results due chiefly to flexure and mechanical hysteresis in the $1\frac{1}{4}$-inch bar linking the crystal to the long screw carriage in the spectrometer, and how this effect is corrected by the use of optical methods (6-inch concave mirror and microscope) at the time of the experiment. The first column gives the value of 2λ between settings for reflections from opposite sides of the crystal planes, after all corrections *except the mirror correction* have been made (the values have not been converted from screw divisions to milliangstroms, however). The second column gives the values after the mirror correction has been applied. These values are in much better agreement than those of the first column.

Table XIII lists the results of the wavelength measurements. These are listed in three different forms: the wavelength of the annihilation radiation, the energy of this radiation, and a comparison of the masses of the positron and the electron. Since there has been, to date, no precise method of obtaining a comparison of the masses of the positron and the electron other than measuring the wavelength of the annihilation radiation, we have interpreted the experiment as a measurement of the mass of the positron. A second measurement of the annihilation radiation has been made by Hedgran and Lind,[47] who determined the energy difference between the annihilation radiation and the 412-kev line following decay of gold 198. Using the most recent measurement of the 412-kev line (described above), the energy of the annihilation radiation can be determined. This energy value, together with the corresponding wavelength value and electron-positron mass difference, is also listed in Table XIII. As a further comparison, the values of $\lambda_c=h/m_-c$ and m_-c^2 obtained by DuMond and Cohen in their most recent least squares adjustment of fundamental constants[25] are given in the table.

[47] Arne Hedgran and David A. Lind, Phys. Rev. 82, 126 (1951).

As a conclusion from these results, we believe it may now be stated that no experimental evidence exists for any difference in the masses of negative and positive electrons greater than a part in ten thousand.

Some additional information can be gleaned from the data for the annihilation radiation line profiles. It is possible to get an idea of the momentum distribution of the centers of mass of the annihilating pairs. This then tells which atomic electrons take part in the annihilation process and to what extent they enter into the reaction.[48]

Since the primary purpose of the experiment was to measure the wavelength of the radiation, we have not attempted an exhaustive study of the shape of the line profile. Such a study would best be undertaken as a separate experiment. It has been possible to calculate

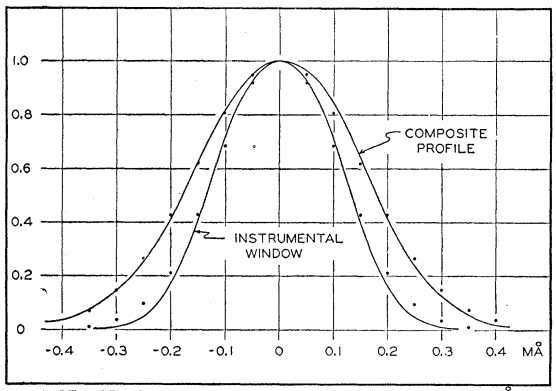

FIG. 18. Showing the effect of Doppler broadening on the observed line profile for the annihilation radiation from copper 64. The composite profile formed by superposition of all observed line profiles is compared with the calculated instrumental window. The dots represent Gaussian functions, $e^{-h^2x^2}$, having the same widths at half-maximum as the solid curves. The composite profile has not been corrected for decay of the source during the time required to obtain a single profile, since such corrections are only slight.

a good approximation to the instrumental "window" profile of the gamma-ray spectrometer[49]; and when the observed line profile is compared with this window curve, the Doppler broadening is readily apparent (see Fig. 18). If we assume that the two curves are Gaussian, then the widths at half-maximum can be combined in quadrature to find the width at half-maximum of the natural line profile. Such an assumption is not, of course, rigorously accurate. Nevertheless, a good estimate of the order of magnitude of the velocities of the centers of mass of the annihilating pairs can be obtained in this manner. Since the calculated instrumental window has a width at half-maximum of 0.270 milliangstrom and the width of the observed line profile at half-maximum is 0.360 milliangstrom, the corresponding width at half-maximum of the natural line profile is 0.238 milliangstrom. Using the nonrelativistic relation for the Doppler shift, this width (one must use half of the above value, or 0.119 milliangstrom in such a calculation) corresponds to a momentum

$$p=9.8\times10^{-3}\ m_0c.$$

This value is in good agreement with the results of the previous experiment performed in this laboratory[46] and with the experiments of DeBenedetti *et al.*[50] This value for the momentum indicates that, for the most part, only the conduction electrons take part in the annihilation process. M electrons might also play a small role in the process. These conclusions are discussed in more detail in references 46 and 50.

X. ACKNOWLEDGMENTS

It is a pleasure to acknowledge the interest in our work and the most helpful criticisms of Professor Richard Feynman, particularly in the case of our studies of iridium 192 in which certain complex line structures looking like very complicated close multiplets appeared. We jumped to the conclusion that these were nuclear lines since they resembled nothing known to us in the x-ray spectrum until Dr. Feynman pointed out that the spacing and intensities of the multiplet could be completely explained as the superposition of two similar symmetrical partially overlapping quadruplets with about 2:1 intensity ratio and a spacing of about 4.9 milliangstroms between them. These two quadruplets are in fact, respectively, the $K\alpha_1$ and $K\alpha_2$ fluorescent lines of lead excited on the edges of the lead slit jaws which we used in the source holder. Each quadruplet consisted of (1) two strong closely adjacent "lines" in the center of the pattern of about equal intensity formed by exciting radiation from the sample falling directly *on* the surface of each slit jaw right at its sharp edge, and (2) two weaker broader and more widely separated fluorescent "lines" formed by exciting radiation which came *through* the jaws from the back. Because of the bevel of the slit jaws, there occurs a point on each at which the depth of penetration for the exciting radiation from behind is optimum for excitation of the greatest fluorescent intensity emerging from the front surface.

The work here reported on tantulum 182 is a continuation of work started by James Brown on this

[48] The half-life of copper 64 was determined in the same manner as was that of gold 198. The final value obtained is 12.77±0.14 hours. This is in good agreement with Silver's value of 12.88 ±0.045 (see reference 45).

[49] The instrumental window was calculated by means of a "fold" taking into account (1) the finite opening of the uranium slit jaws, (2) the penetration of the radiation into the edges of the slit jaws, and (3) the estimated window ascribable to the crystal (intrinsic diffraction pattern and aberration of focusing) as determined by measurements on very thin sources with spectrally very narrow lines (e.g., cesium 137).

[50] DeBenedetti, Cowan, and Konneker, Phys. Rev. **76**, 440 (1949); DeBenedetti, Cowan, Konneker, and Primakoff, Phys. Rev. **77**, 205 (1950).

isotope with the 2-meter crystal spectrometer in 1949 and 1950, which formed part of his thesis for the doctorate. The first mentioned of the two sources, the narrower and the weaker of the two, was the one used by him. Actually all the wavelengths have been remeasured with the second source because certain changes in the spectrometer in the meanwhile have rendered the applicability of our present calibration to this older data too uncertain. Nevertheless, Brown's pioneering study on this isotope has been of the greatest value to us, and it is a pleasure to acknowledge here our indebtedness to him.

PHYSICAL REVIEW VOLUME 88, NUMBER 4 NOVEMBER 15, 1952

Penetration and Diffusion of X-Rays: Calculation of Spatial Distributions by Semi-Asymptotic Methods*

L. V. SPENCER
National Bureau of Standards, Washington, D. C.
(Received June 20, 1952)

Methods are presented for calculating x-ray spectra in an infinite homogeneous medium. These methods are particularly useful for calculating spectra at great distances from the radiation source. The transport equation is solved numerically by characterizing angular and spatial distributions with a small number of suitable parameters. Attention is called to a mathematical technique which is extremely useful for this purpose, whereby a function may be approximated from a knowledge of moments, derivatives, or values. Sample numerical applications include spectral intensities at various distances from a plane monodirectional 10.22-Mev x-ray source in Pb and a plane monodirectional 5.11-Mev source in Fe.

I. INTRODUCTION

THE very deep penetration of photons which experience multiple Compton scattering[1] has been studied previously in a number of papers.[2–4] These treatments—all completely analytic—have been designed to yield information about the asymptotic form of the x-ray penetration law. In this paper we shall present a numerical approach which makes use of these asymptotic penetration laws; therefore, in Appendix A we summarize these earlier results and discuss briefly some unpublished work of the same kind.

The complicated nature of actual x-ray cross sections militates strongly against the usefulness of purely analytical methods in finding realistic spectral intensities in specific situations. Numerical methods hold much more promise. One such numerical method has been presented[5–7] which relies an expansions in suitable spatial and directional polynomial systems. The diffusion equation is reduced through these expansions to a form suitable for ordinary numerical integrations. This polynomial method has proved very useful for penetrations up to 16–24 mean free paths of the hardest spectral component; but it is in no sense asymptotic since the burden of the numerical integrations tends to increase rapidly with the penetration.

We present here a method for numerical calculations which might be called "semi-asymptotic." It is capable of yielding as much information as the polynomial method, while the numerical work involved is nearly independent of the penetration. This method relies upon a Fourier-Laplace transformation in the spatial variable. In Sec. II the diffusion equation is presented and is reduced, through this spatial transformation and through integrations over photon directions, to an interlinked system of integral equations. Section III describes schematically an approach to the solution of this system. Section IV presents the method which was actually used. The success of this method is largely due to a new mathematical technique for approximating functions. In order to preserve continuity of thought, this technique is described in Appendix B rather than in the body of the text. In Sec. VII the inversion of the Fourier-Laplace transform is discussed. The details of the inversion are given in Appendix C.

The results of actual calculations for the following three problems are presented and discussed in Sec. VIII: (1) a plane monodirectional 10.22-Mev source in Pb; (2) a plane monodirectional 5.11-Mev source in Fe; (3) a plane isotropic 5.11-Mev source in Fe. Spectral intensities are given for penetrations up to 160 mean free paths in the first case and 50 mean free paths in

* Work supported by the ONR.

[1] At the low energy end of the spectrum, where the energy shift of the scattered photons can be disregarded or treated as a small correction, the diffusion of photons has been studied by S. Chandrasekhar (*Radiative Transfer*, Oxford University Press, London, 1950), but without specific reference to very deep penetrations. At the very high energy end, where large amounts of x-rays are regenerated by secondary electrons, a full development of the shower theory is required. Pair production will be treated here as a mechanism for outright absorption. (The results of this paper can be applied to the tail end of showers.)

[2] Bethe, Fano, and Karr, Phys. Rev. **76**, 538 (1949).

[3] U. Fano, Phys. Rev. **76**, 739 (1949).

[4] Fano, Hurwitz, and Spencer, Phys. Rev. **77**, 425 (1950).

[5] L. V. Spencer and U. Fano, Phys. Rev. **81**, 464 (1951).

[6] L. V. Spencer and U. Fano, J. Research Natl. Bur. Standards **46**, 446 (1951).

[7] L. V. Spencer and Fannie Stinson, Phys. Rev. **85**, 662 (1952).